ELSEVIER

Thermochimica Acta 280/281 (1996) 223–236

thermochimica acta

Crystal nucleation and growth in soda-lime–silica glasses close to the $Na_2O \cdot 2\,CaO \cdot 3\,SiO_2$ (NC_2S_3) composition. Crystal nucleation kinetics in the stoichiometric NC_2S_3 composition[1]

C.J.R. González Oliver [a,*], P.F. James [b]

[a] *(Conicet)-Centro Atómico Bariloche, Av.E. Bustillo, km 9.5, (8400) S.C. de Bariloche, Río Negro, Argentina*

[b] *Department of Engineering Materials, University of Sheffield, Sir R. Hadfield Building, Mappin Street, Sheffield, S1 4DU, UK*

Abstract

For the stoichiometric NC_2S_3 glass (G16) non-steady-state crystal nucleation was found for temperatures lower than 600 °C. For the nucleation range similar nucleation frequencies (I) were observed on using either double-stage or single-stage heating schedules. The interfacial energy (σ) and pre-exponential factor in the nucleation expression were determined using I, η (viscosity), and calculated ΔG (free energy driving force) values estimated independently. A reasonable value of 193 mJ m^{-2} was obtained for σ but the pre-exponential factor was much greater than predicted by theory.

Keywords: Crystal growth; Crystal nucleation; Crystal nucleation kinetics; DTA; Interfacial energy; Soda-lime–silica glass; Stoichiometric glass; Viscosity

1. Introduction

Glass ceramics are obtained by the controlled crystallisation of glasses [1]. Studies of crystal nucleation and growth kinetics in glasses are important in the understanding of glass ceramic formation and because of the relatively slow molecular rearrangements

* Corresponding author.

[1] Dedicated to Professor Hiroshi Suga.

SSDI 0040-6031(95)02644-4

and diffusion, these processes can be conveniently studied in glass-forming systems [2]. Glass ceramic formation in the soda-lime–silica system [3–5] has previously been studied because of the relatively inexpensive raw materials required to prepare the glasses and also as a result of the high volume crystal nucleation rates in the compositions $Na_2O{\cdot}2CaO{\cdot}3SiO_2$ (NC_2S_3) and $2Na_2O{\cdot}1CaO{\cdot}3SiO_2$ (N_2CS_3). The influence of water content [6] and of platinum [7,8] additions on the rates and mechanisms of crystal nucleation and growth in (NC_2S_3) glasses have been previously determined. Several groups [9,10] have recently investigated these glasses with the DTA technique and from analysis of their kinetics, the activation energy for crystallization, E_c, was estimated to range from about 300 to 370 kJ mole^{-1}. Further, from such analysis [10] it was possible to estimate the crystal nucleation vs. temperature curve, which agrees reasonably well with our *measured* crystal nucleation rates for NC_2S_3 glasses [4, 6, 8, 11, 12].

In the present paper an analysis is made of the steady-state crystal nucleation for the stoichiometric NC_2S_3 glass. The effects of changing the base composition on the crystal nucleation (preliminary results presented in Refs. [2, 11, 12]) and growth kinetics [4] will be given in later publications.

2. Experimental

The glasses were prepared from analytical reagent grade carbonates of sodium and calcium and for most of the melts (except G 16) silica sand containing 0.009 wt% total iron oxides and 0.05 wt% alumina impurities was used. Glass G 16 was prepared with a higher purity SiO_2 (Sil–quartz) in order to check the possible effects of the trace elements on nucleation and growth rates. Melting was carried out in Pt 2% Rh crucibles in an electric furnace at 1400 °C for 5 h in air (including stirring with a platinum blade for 2 h). All glasses were melted using a similar operating schedule. After melting, the glass was pressed between steel plates to obtain a fast quench and to avoid surface crystallization.

The nucleation rates were determined from the number of particles (spherulites) per unit volume (N_v) in heat-treated glass samples. Sections cut through the samples were ground, polished, lightly etched in dilute HF solution, and examined by reflected light microscopy (OM) and scanning electron microscopy (SEM). Further experimental details are given elsewhere [4, 6, 11, 13]. N_v was determined from

$$N_v = (2/\pi) N_A \langle 1/b \rangle \tag{1}$$

where N_A is the number of particle intersections per unit area and $\langle 1/b \rangle$ is the mean value of the reciprocals of the measured diameters for all circular intersections [13, 14]. For constant particle size a simpler equation

$$N_v = N_A/b \tag{2}$$

was used where b is the largest circular cross-section diameter. The nucleation rates were obtained from the N_v values for samples heated for a series of times at the nucleation temperature. After nucleation further heat treatment was carried out at

a higher temperature (about 730°C) for a short time (usually only a few minutes and depending on the nucleation treatment) to grow the crystals to sizes observable with the optical microscope. This procedure is referred to as the double-stage (DS) heat treatment [2, 13]. A single-stage treatment was used for determinations of nucleation rates with the scanning electron microscope (SEM).

Viscosity (η) data were obtained with a penetration viscometer and a beam-bending apparatus at lower temperatures and with a rotating cylinder viscometer at higher temperatures [4, 6]. The equipment was calibrated with a standard glass (NBS 710) which has a known viscosity–temperature relationship.

DTA (differential thermal analysis) runs were carried out, in air, in a Standata 625 (UK) apparatus at 10°C min^{-1} heating rate using powdered α-Al_2O_3 as reference. By measuring the areas under the peaks and calibrating the analyser with AR NaCl and AR NaF, the heats of crystallization (ΔH_c at T_c) and of melting (ΔH_f at T_m) were estimated. The materials for examination were crushed in a percussion mortar and ground in an agate mortar to 300 B.S. mesh size.

3. Results

3.1. Glass Compositions

The glass compositions used are listed in Table 1. The wet chemical analysis (W.A.) for glasses G2 and G16 indicates that they are close in composition. These glasses were characterized by electron probe microanalysis (EPMA). In Table 1 it can be observed that a similar trend is obtained for the nominal compositions and those determined by EPMA.

3.2. Nucleation rates viscosity, and DTA data

The nucleation kinetics for G16 were analysed from optical micrographs of samples subjected to double-stage (DS) heat treatments. In addition, the number of crystals

Table 1
Nominal (N) oxide compositions (in mol%). Values between square brackets correspond to wet chemical analysis [W.A.]. Between round brackets are EPMA results (E)

Glass code	Type of value	Na_2O	CaO	SiO_2
G2	N	16.66	33.33	50.00
	W.A.	[16.3]	[33.1]	[50.6]
G16	N	16.66	33.33	50.00
	W.A.	[16.06]	[33.21]	[50.73]
	E	(16.1)	(33.2)	–
G17	N	16.66	33.33	50.00
	E	(15.9)	(33.3)	–

produced after a single nucleation stage (SS) nucleation and growth heat treatment were measured using SEM. As in the case of the optical microscopy determinations, random cross-sectional planes of the etched glass samples were analysed to obtain N_v (see above). The number of crystals per unit volume are shown in Figs. 1 and 2 as a function of time for different nucleation temperatures. The steady-state nucleation rates and "approximated" nucleation rates (N_v/t for t equal to 40 min) determined from optical microscopy and from the SEM analysis are presented in Fig. 3 and Table 2.

Appreciable non-steady-state nucleation is present at lower temperatures (Fig. 1). The slopes of the linear part of the plots (at longer times) give the steady-state nucleation rates (I_0), and the intercepts (t_0) with the time axis are related to the induction times. Both I_0 and t_0, were determined from least square analysis of the linear region of the plots. Appreciable intercepts occur at 607°C ($t_0 = 17$ min) and at 585°C ($t_0 = 37$ min). The steady-state nucleation rates show a maximum ($\log_{10} I_0 \simeq 11.652$) at about 605°C. It is interesting to compare the steady-state values with the approximated rates calculated from N_v/t where $t = 40$ min is the nucleation time. From Fig. 3 the

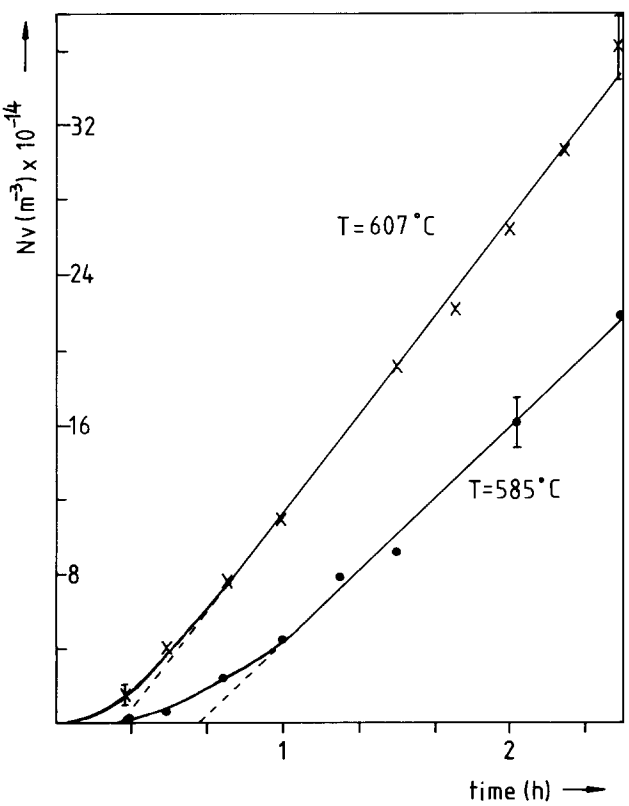

Fig. 1. Crystal nucleation densities (N_v) vs. time at $T = 585$°C (●) and $T = 607$°C (×) for glass G16, double-stage (DS) treatments (growth at 730°C) using optical microscopy. Error bars represent 10% relative uncertainty ($\Delta N_v/N_v \times 100 = 10\%$).

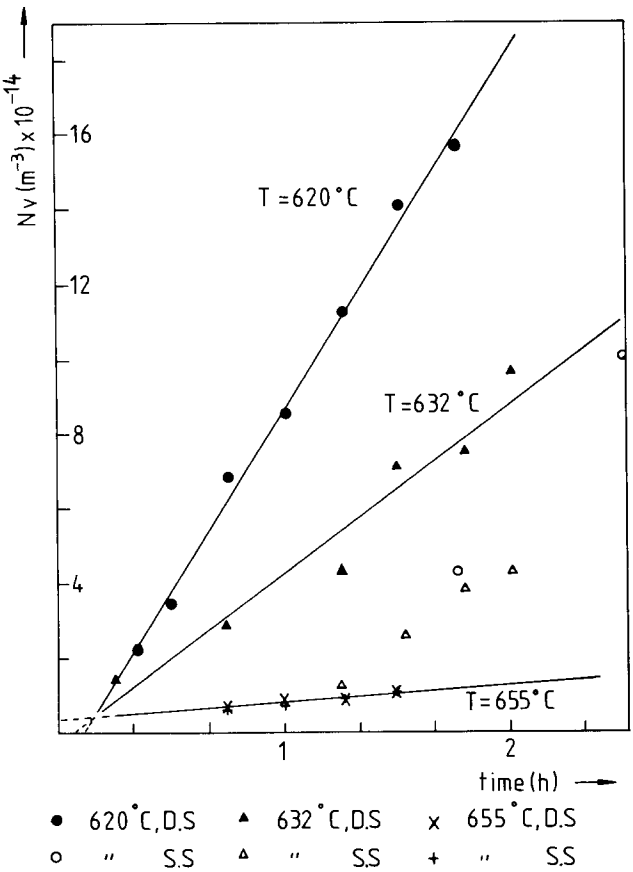

Fig. 2. Crystal nucleation densities (N_v) vs. time for glass G16; 620°C (●), 632°C (▲), 655°C (×): double-stage (DS) treatments using optical microscopy. 620°C (○), 632°C (△), 655°C (+): single-stage (SS) treatments (using SEM).

agreement between both is good for temperatures higher than about 610°C. The lower the nucleation temperature, below 610°C, the greater is the underestimation in I_0 using $N_v/t(t = 40\,\text{min})$ and this effect is directly related to non-steady-state nucleation behaviour. The nucleation curve ($N_v/t, t = 40$ min) for G2 (given in [4] and [11]) nearly coincides with that for G16 (Fig. 3), which confirms the close chemical composition of the glasses (see Table 1).

The SEM results are also plotted in Figs. 2 and 3 and the agreement of the steady-state *rates* from the single-stage (SS) method with the double-stage (DS) method is good (see Table 2). However, the *number* of crystals obtained with the SEM is never larger than the number obtained from the DS method; the values only become comparable at the higher nucleation temperatures (i.e. at about 655°C and higher). The lower number of particles determined by the SEM results, as will be demonstrated

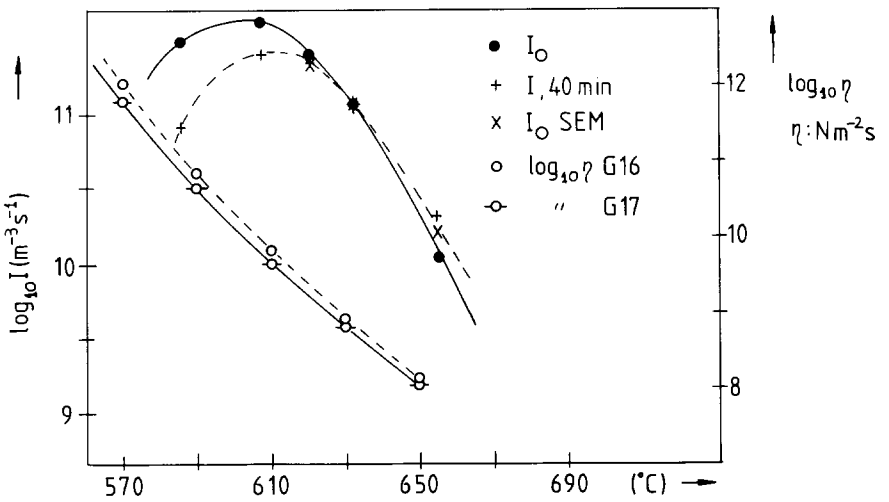

Fig. 3. Steady-state nucleation rates I_o (●) and approximated nucleation rates (+) after 40 min using (N_v/t) where $t = 40$ min. for glass G16 as a function of temperature (optical microscope values); SEM values are also plotted (×). Viscosity curves according to Fulcher parameters (Table 3) for glasses G16 (○) and G17 (–○–).

Table 2
Nucleation densities for glass G16

Experimental technique	T/°C	Steady state nucleation rate in nuclei/($m^{-3}s^{-1}$)		Approximated nucleation rate after 40 min in nuclei/($m^{-3}s^{-1}$)		Intercept with time axis (see text)/min
		$I_o \times 10^{-11}$	$\log_{10} I_o$	$(I = N_v/t) \times 10^{-11}$	$\log_{10} I$	
Double stage heat treatment (OM)	585	3.204	11.506	0.833	10.921	37.48
	607	4.374	11.641	2.542	11.405	17.08
	620	2.722	11.435	2.271	11.356	7.02
	632	1.263	11.101	1.167	11.067	4.24
	655	0.121	10.081	0.271	10.433	−50.8
Single stage heat treatment (SEM)	620	2.162	11.335	–	–	–
	632	1.167	11.067	–	–	–
	655	0.178	10.251	–	–	–

shortly, from the very small size of the crystals for a typical nucleation time of 100 min. The smaller the crystals, the more difficult they are to detect by SEM in a random cross-sectional plane through the specimen. In fact at the higher temperatures, where the crystal growth rates are higher, both methods give similar results. The results suggest that there is a systematic error in the measured N_v determined by the SEM, which at a given temperature is fairly constant with heat treatment time.

From nucleation theory the size of the critical nucleus increases with increasing temperature. Hence, critical nuclei at the lower (nucleation) temperatures (570 to 690°C) are smaller than the critical size at the upper (growth) temperatures (720 to 730 °C) and should dissolve when the temperature is raised to the growth temperature. In fact, during the nucleation treatment the nuclei *grow* to appreciable sizes and can exceed the critical size at the growth temperature. The crystal size vs time plots indicate appreciable incubation effects up to 640 °C. For temperatures of 620, 632 and 655 °C and after times of, respectively, 25, 19 and 0 min the growth rates reach constant values of 0.028, 0.065 and 0.240 μm min^{-1}. Thus, for a nucleation time of 100 min the corresponding radii expected for the nuclei first formed are 2.11 μm (= (100 − 25) × 0.028) at 620 °C, 5.2 μm at 631 °C and 24 μm at 655 °C. The size of the critical nuclei for glass G16 cannot be accurately calculated at this stage because the interfacial free energy, σ, is not known (it will be determined from the steady state nucleation data later). The critical size assuming a spherical nucleus is approximately given by

$$r(T) = 2\sigma V_m T_m / \Delta H_f (T_m - T) \tag{3}$$

where σ, V_m, T_m and ΔH_f are the interfacial free energy (J m^{-2}), the molar volume of the crystal phase (m^3), the melting temperature (K) and the heat of fusion (J $mole^{-1}$), respectively. Assuming that changes in σ and V_m with temperature are negligible, the ratio $r(730\,°C)/r(620\,°C)$ may be calculated as 1.20. Then, if as an estimate a value of 10 Å is taken [13] for the critical radius at 620 °C, the critical radius at 730 °C, is about 12 Å. Consequently, the great majority of the crystals should have reached larger sizes than the critical size corresponding to the growth temperature *before* the second-stage treatment. A second assumption in the DS method is that the nucleation rate at the growth temperature is negligible and this clearly holds for the present glasses.

Electron micrographs of G16 heated at 632 °C for 92 min reveal nearly perfect spherical morphology. However, for the same glass heated at lower temperatures, for example at $T = 620$ °C for 75 min, the crystals have a more polyhedral shape. The NC_2S_3 crystals contain bands which were tentatively assigned to planar imperfections like stacking faults [7]. The origin of such faults was related [7] to the volume change associated to the polymorphic crystal phase transition (rhombohedral high form to hexagonal low form) at around 475 °C. That is, the crystals are nucleated and grown at temperatures higher than 475 °C where the stable phase is the rhombohedral high form and subsequently cooled through the transition temperature and are obtained the hexagonal low form phase.

Viscosity data for G16 was obtained between 570 and 650 °C. The Fulcher equation was fitted to the low temperature data for G16 and to the high temperature range data of the glass G2; here it was assumed that the viscosities of G16 and G2 were close at high temperatures [4, 11]. The corresponding Fulcher parameters are listed in Table 3 and the associated viscosity curve for G16 is shown in Fig. 3 together with the curve for G17. From the Fulcher equations for glasses G2, G16 and G17, the temperatures corresponding to $\log_{10}\eta = 12$ ([η] in Pa s) are obtained at 565, 570 and 566°C, respectively. G16 is slightly more viscous than either G2 or G17 at low temperatures; however, the difference in the $\log_{10}\eta$ values is never larger than about 0.3.

Table 3
Fulcher parameters ($\log_{10}\eta = A + B/(T - T_o)$) for the different glasses

Glass code	Fulcher parameters			Temperature/°C at which $\log_{10}\eta = 12$
	A	B	T_o/°C	
G2	−4.86	4893	274	564
G16	−4.37	4225	312	570
G17	−4.44	4339	302	566

The DTA traces for G2, G16 and G17 are similar. For instance for glass G2, for the heating cycle, DTA gives [4, 11] an endothermic dip at 579 °C (DTA T_g, defined as shown schematically in Fig. 4), an exothermic crystallization peak at about 700 °C and an endothermic melting peak at 1291 °C. On the cooling cycle, after crystallization, the polymorphic crystal phase transition is also detected for each glass (rhombohedral high form to hexagonal low form) at around 475 °C. The DTA T_g values (see Table 4) show

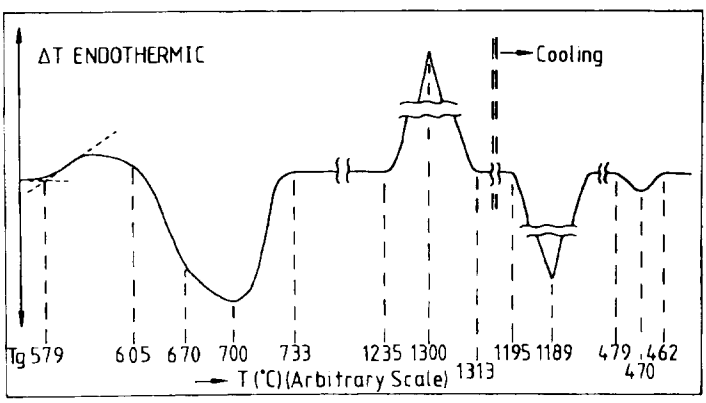

Fig. 4. DTA trace for glass G2 (300 mg); reference material Al_2O_3 (300 mg); ΔT sensitivity 100 μV full scale-deflection; heating and/or cooling rate 10°C min^{-1}.

Table 4
DTA data and fixed growth rates for the different compositions

Glass code	ΔH_c/(kJ $mole^{-1}$)	ΔH_f/(kJ $mole^{-1}$)	DTA T_g/°C	T_m/°C	Growth rates at 675 °C/(μm min^{-1})
G2	53.2 ± 2.8	86.3 ± 4.3	579	1291	0.58
G16	56.5 ± 3.0	86.2 ± 4.2	582.5	–	–
G17	–	–	578	–	–

similar trends to those quoted for temperatures at which $\log_{10}\eta$ is 12. The heats of crystallization (ΔH_c), and fusion (ΔH_f) are listed in Table 4 and within experimental error the values for G16 are the same as that obtained for G2 [4, 11].

4. Discussion

4.1. Theoretical considerations

According to classical theory the crystal nucleation rate may be written as [2, 4, 15]:

$$I = A\exp\left(-\frac{W^*}{RT}\right)\exp\left(-\frac{\Delta G_D}{RT}\right) \tag{4}$$

where ΔG_D is the kinetic *free* energy barrier per mole, W^* is the thermodynamic free energy barrier to nucleation per mole, k and h are the Boltzmann and Planck constants and R is the gas constant. For a spherical nucleus

$$W^* = 16\pi\sigma^3 V_m^2/3\,\Delta G^2 \tag{5}$$

where ΔG is the bulk free energy change per mole in the transformation, σ the interfacial free energy per unit area and V_m is the molar volume of the crystal phase. A, the pre-exponential factor is, to a good approximation, given by

$$A = n_v kT/h \tag{6}$$

where n_v is the number of formula units per unit volume of liquid. If the diffusion coefficient

$$D = D_o\exp\left(-\frac{\Delta G_D}{RT}\right) \tag{7}$$

and the viscosity (η) are related through the Stokes–Einstein equation, Eq. (8)

$$D\eta = kT/3\pi a_o \tag{8}$$

(a_o is the effective atomic diameter) we obtain

$$\exp\left(-\frac{\Delta G_D}{RT}\right) = \frac{D}{D_o} = \frac{kT}{3\pi a_o D_o \eta} \tag{9}$$

Substituting back in Eq. (4)

$$I\eta = \frac{n_v kT}{3\pi\lambda^3}\exp\left(-\frac{W^*}{RT}\right) = A_C T\exp\left(-\frac{W^*}{RT}\right) \tag{10}$$

where $D_o = v\lambda^2 \simeq (kT/h)\lambda^2$, v is the frequency for atomic transfer from the liquid to the crystal, λ is the jump distance for diffusion, and we assume that λ and a_o are approximately equal. A_C is given in terms of the pre-exponential factor $A \simeq n_v kT/h$ by

$$A_C = \frac{Ah}{3\pi\lambda^3 T} \tag{11}$$

From Eq. (10) and the expression for W^* it follows that a plot of $\ln(I\eta/T)$ vs. $1/\Delta G^2 T$ should be linear, the slope and appropriate intercept enabling the interfacial energy σ and the pre-exponential factor to be calculated.

Let us examine in more detail the meaning of Eq. (9). According to Oishi et al. [16] for soda-lime glasses the apparent activation enthalpy for diffusion (ΔH_D) of oxygen increases rapidly in the transformation range. From Eq. (9) the same trend should be observed for ΔH_η, the activation energy for the shear viscosity. For many systems the viscosities as a function of temperature are better described by a Fulcher equation than an Arrhenius equation with a constant activation enthalpy. By comparing $\eta = \eta_o \exp[\Delta G_\eta/RT]$ (where the *free* energy is $\Delta G_\eta = \Delta H_\eta - T\Delta S_\eta$, $\Delta H_\eta = [\partial(\Delta G_\eta/T)/\partial(1/T)]_P$, $\Delta S_\eta = [-\partial \Delta G_\eta/\partial T]_P$ and also ΔG_η, ΔH_η and ΔS_η are now considered as functions of temperature) with the Fulcher expression $\log_{10}\eta = A + B/(T - T_o)$ we obtain

$$\Delta H_\eta = B' R T^2/(T - T_o)^2 \tag{12}$$

$$\Delta S_\eta = B' R T_o/(T - T_o)^2 - A' R + R \ln \eta_o \tag{13}$$

$$\Delta G_\eta = RT[B'/(T - T_o) + A' - \ln \eta_o] \tag{14}$$

where $A' = 2.30\,A$ and $B' = 2.30\,B$. It can be seen that ΔH_η *increases* with decreasing T. For example with $T_o = 300\,^\circ\mathrm{C} = 573\,\mathrm{K}$, for $T = 873$, 853, 833 and 803 K the values $\Delta H_\eta/B'R = T^2/(T - T_o)^2$ are 8.47, 9.28, 10.26 and 12.19, respectively.

Let us examine the variation of ΔG_η with T. From Eq. (14) we have:

$$\frac{d\Delta G_\eta}{dT} = -[B' R T_o/(T - T_o)^2 - A' R + R \ln \eta_o] \tag{15}$$

Clearly, for T approaching T_o the derivative is *negative* showing that ΔG_η increases with decreasing temperature. However, for the temperature range of interest, say from 750 to 950 K, the variation of ΔG_η is not obvious because of the $A'R - R \ln \eta_o$ term. Using typical values for the Fulcher constants ($A = -4$, $B = 4 \times 10^3$ and $T_o = 300\,^\circ\mathrm{C} = 573\,\mathrm{K}$) at $T = 850\,\mathrm{K}$ the first term between brackets in Eq. (15) is $-69\,R$. A reasonable estimate of η_o appears to be about 10^{-6} on the basis of the analysis of Litovitz and Macedo [17] for B_2O_3 glass (see also [20] for other glasses). The second term ($R[\ln \eta - A']$) in Eq. (15) then becomes $+4.6\,R$. Therefore the activation *free* energy for viscosity should increase as T decreases. From Eq. (9) the activation *free* energies for diffusion and viscosity should follow a similar trend with falling temperature. Furthermore, the diffusion coefficients calculated from Eq. (9) agree with the *measured values* to within an order of magnitude. Hence it appears that the approximations involved in the derivation of Eq. (9) are reasonable.

4.2. Glass G16

For glass G16 the steady state I_o and approximated nucleation rates N_v for 40 min (using the values read from the continuous curves in Fig. 3 and the data in Table 2) were employed together with the viscosity data (Table 3) to test Eq. (10).

The ΔG values previously calculated for G2 [4, 11] were used due to the very similar thermal properties of both glasses (see Table 4). The $\ln[I\eta/T]$ vs $1/\Delta G^2 T$ plots are shown in Fig. 5. All the steady state values are on a good straight line, giving σ as 191 mJm^{-2} and $\log_{10} A$ as 103.5. The straight line indicates good agreement with the theory over the temperature range considered assuming a constant σ independent of temperature but allowing ΔG_D to increase with decreasing temperature in accordance with the viscosity. However, as observed previously for G2 [4, 11] the pre-exponential factor is too large when compared with the theoretical value ($\log_{10} A \simeq 40.9$). It should be noticed that the values for σ and $\log_{10} A$ for G16 are somewhat higher than those previously obtained for G2 ($\sigma = 180$ mJ m^{-2}; $\log_{10} A = 90$). This is probably because of the small difference in composition between G16 and G2.

Fig. 5 also shows that the approximate nucleation rates (using the N_v for 40 min) only fall on the straight line above 605 °C. This emphasizes the importance of using the steady state nucleation rates in these plots.

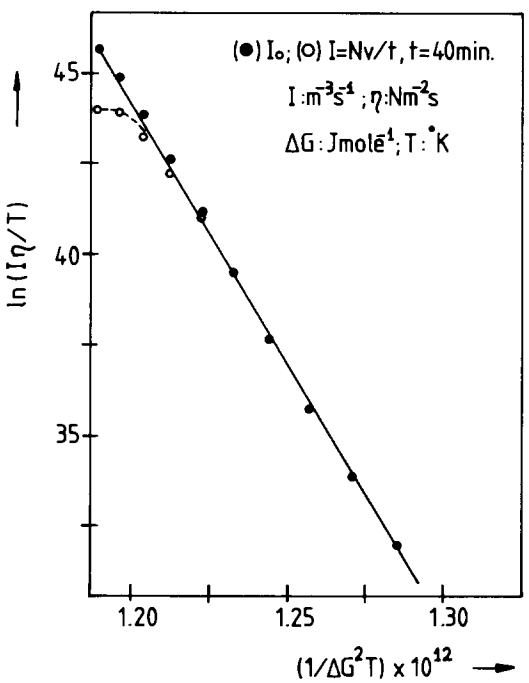

Fig. 5. Ln($I\eta/T$) as a function of ($1/\Delta G^2 T$) for glass G16.

It is interesting to compare the present result with the σ calculated from the empirical equation obtained by Matusita and Tashiro [18] in analysing alkali disilicate glasses:

$$\sigma = 0.45 \frac{\Delta H_f}{N_A^{1/3}} \left(\frac{\rho_s}{M} \right)^{2/3} \tag{16}$$

where N_A is Avogadro's number, ρ_s is the solid density (2.80 g cm^{-3} for crystalline NC_2S_3) and M is the molecular weight (354.42 g for NC_2S_3). The value σ is 193 mJ m^{-2} which compares well with the value for G16 but is higher than that obtained for G2.

The nucleation intercepts (t_o) in Table 2 for G16 will now be analysed in terms of $\tau = (6/\pi^2)t_o$. James [13] has shown that the incubation time, τ, can be expressed as

$$\tau = \frac{16 h \lambda^2 \sigma N_A^2}{\hbar^2 V_m^2 \Delta G_V^2} \exp\left(\frac{\Delta G_D}{RT} \right) \tag{17}$$

where ΔG_V is the driving force per unit volume ($\Delta G = V_m \Delta G_V$). Also he related τ to η using the Stokes–Einstein equation as follows

$$\tau \simeq \frac{48 \sigma \lambda^5 \eta N_A^2}{V_m^2 \Delta G_V^2} \tag{18}$$

We have effected *four different plots*: $\ln(\tau \Delta G_V^2)$ vs $1/T$ according to Eq. (17), $\ln \tau$ vs $1/T$, $\ln[\tau \Delta G_V^2/\eta]$ vs $1/T$ according to Eq. (18), and $\ln \eta$ vs $1/T$. From the first plot the slope gave an apparent activation enthalpy ΔH_D of 327 kJ mole^{-1}. So far the agreement between experiment and Eq. (17) appears reasonable. However, from a similar analysis the apparent activation enthalpy ΔH_η for the shear viscosity was 820 kJ mole^{-1}. Nevertheless it is interesting to calculate the predicted absolute τ value from Eq. (18). For example at 585 °C using the measured viscosity ($\log_{10}\eta = 11.1$) and $\lambda = 7 \times 10^{-10}$ m we obtained $\tau = 2.3 \times 10^4$ s which is 17 times *greater* than the measured τ (1.37×10^3 s). For theory and experiment to agree the viscosity at 585 °C should be $\log_{10} \eta = 9.87$ which is outside the experimental error in the measurements. However, it is known that the Stokes–Einstein equation may be in error by about an order of magnitude at temperatures near the transformation range. On this basis, and in view of the uncertainties in the estimation of the quantities in Eq. (18), the agreement between theory and experiment is reasonable.

5. Summary and conclusions

For the stoichiometric NC_2S_3 glass G16 the nucleation densities (N_v/t) for constant heat treatment time (40 min), at a series of temperatures, were found to be a good measure of the steady-state nucleation rates I_o, particularly at temperatures higher than the maximum in nucleation. At such temperatures "steady-state" conditions applied and the nucleation rate I was constant with time, whereas at much lower

temperatures below the maximum, non-steady-state conditions increasingly applied with decrease in temperature, and N_v/t values underestimated the steady-state nucleation rates I_0. Classical nucleation theory provides a good fit to the experimental nucleation rates when the kinetic *free* energy barrier, ΔG_D, is allowed to increase with decreasing temperature. The diffusion term involving ΔG_D was assumed to have the same temperature-dependence as the viscosity. The thermodynamic driving force, ΔG, which was needed in the analysis, was determined from measurements of the heat of fusion ΔH_f and the difference in specific heats of the crystal and liquid phases ΔC_p. From the fit between theory and experiment the crystal–liquid interfacial free energy was found to be 191 mJ m^{-2}. This value compares well with 193 mJ m^{-2} obtained from Matusita's empirical expression [18].

The pre-exponential factor A is found too large when compared to the theoretical value. A possible explanation of such a discrepancy may be a temperature-dependent σ, as discussed by James [19].

In relation to the nucleation intercepts a good fit to Eq. (17), discussed in [13], was obtained and the apparent activation energy (ΔH_D) was 327 kJ mole^{-1}. The predicted incubation times (τ) were 17 times greater than measured but since the Stokes–Einstein relationship, relating diffusivity and viscosity, may be in error by a factor of ten, the agreement between theory and experiment appears reasonable.

Acknowledgements

C.J.R. González Oliver wishes to thank Messrs. R. Bacon and E. Crossland (University of Sheffield) for technical assistance, and the Editing Staff of the Centro Atómico Bariloche for help in preparing this paper. He acknowledges the revision of this article by Professor J. Sestak.

References

[1] P.W. MacMillan, Glass Ceramics, Academic Press, London and New York, 1964.
[2] P.F. James, Adv. Ceram. Vol. 4, Am. Ceram. Soc., 1982, 1.
[3] Z. Strnad and R.W. Douglas, Phys. Chem. Glasses, 14 (1973) 33.
[4] C.J.R. González Oliver, Ph.D. Thesis, University of Sheffield, UK, 1979.
[5] A.M. Kalinina, V.N. Filipovich and V.M. Fokin, J. Non-Cryst. Solids, 38/39 (1980) 723.
[6] C.J.R. González Oliver, P.S. Johnson and P.F. James, J. Mater. Sci., 14 (1979) 1159.
[7] C.J.R. González Oliver and P.F. James, J. Micros., (Oxford) 119 (1980) 73.
[8] C.J.R. González Oliver and P.F. James, Adv. Ceram., Vol. 4, Am. Ceram. Soc., 1982, 49.
[9] N. Koga, J. Šesták and Z. Strnad, Thermochim. Acta, 203 (1992) 361.
[10] X.J. Xu, C.S. Ray and D.E. Day, J. Am. Ceram. Soc., 74(5) (1991) 909.
[11] C.J.R. González Oliver and P.F. James, J. Non-Cryst. Solids, 38/39 (1980) 699.
[12] C.J.R. González Oliver, A.M. Ramsden, E.G. Rowlands and P.F. James, Proc. VII Int. Congr. Ceram., ATAC, 1979, Buenos Aires, p. 434.
[13] P.F. James, Phys. Chem. Glasses, 15 (1974) 95.
[14] R.T. DeHoff and F.N. Rhines, Quantitative Microscopy, McGraw-Hill, NY, 1968.
[15] E.D. Zanotto and P.F. James, J. Non-Cryst. Solids, 74 (1985) 373.

[16] Y. Oishi, R. Terai and H. Ueda, in A.R. Cooper and A.H. Heuer (Eds.), Mass Transport Phenomena in Ceramic Materials, Plenum Press, NY, London, 1975.
[17] T.A. Litovitz and P.C. Macedo, J. Chem. Phys., 42(1) (1965) 245.
[18] K. Matusita and M. Tashiro, J. Non-Cryst. Solids, 11 (1973) 471.
[19] P.F. James, J. Non-Cryst. Solids, 73 (1985) 517.
[20] C.T. Moynihan, J. Am. Ceram. Soc., 76(5) (1993) 1081.